JACS
JOURNAL OF THE AMERICAN CHEMICAL SOCIETY

Subscriber access provided by American Chemical Society

Article

Thermodynamics of Folding, Stabilization, and Binding in an Engineered Protein–Protein Complex

Vildan Dincbas-Renqvist, Christofer Lendel, Jakob Dogan, Elisabet Wahlberg, and Torleif Hrd

J. Am. Chem. Soc., **2004**, 126 (36), 11220-11230• DOI: 10.1021/ja047727y • Publication Date (Web): 20 August 2004

Downloaded from http://pubs.acs.org on April 1, 2009

More About This Article

Additional resources and features associated with this article are available within the HTML version:

- Supporting Information
- Access to high resolution figures
- Links to articles and content related to this article
- Copyright permission to reproduce figures and/or text from this article

View the Full Text HTML

ACS Publications
High quality. High impact.

Journal of the American Chemical Society is published by the American Chemical Society. 1155 Sixteenth Street N.W., Washington, DC 20036

J|A|C|S
ARTICLES
Published on Web 08/20/2004

Thermodynamics of Folding, Stabilization, and Binding in an Engineered Protein−Protein Complex

Vildan Dincbas-Renqvist,[†] Christofer Lendel,[†] Jakob Dogan,[†] Elisabet Wahlberg,[†] and Torleif Härd*[,‡]

Contribution from the Department of Biotechnology, Royal Institute of Technology (KTH), S-106 91 Stockholm, Sweden, and Department of Medical Biochemistry, Göteborg University, Box 440, S-405 30 Göteborg, Sweden

Received April 20, 2004; E-mail: torleif.hard@medkem.gu.se

Abstract: We analyzed the thermodynamics of a complex protein−protein binding interaction using the (engineered) Z_{SPA-1} affibody and it's Z domain binding partner as a model. Free Z_{SPA-1} exists in an equilibrium between a molten-globule-like (MG) state and a completely unfolded state, wheras a well-ordered structure is observed in the $Z{:}Z_{SPA-1}$ complex. The thermodynamics of the MG state unfolding equilibrium can be separated from the thermodynamics of binding and stabilization by combined analysis of isothermal titration calorimetry data and a separate van't Hoff analysis of thermal unfolding. We find that (i) the unfolding equilibrium of free Z_{SPA-1} has only a small influence on effective binding affinity, that (ii) the $Z{:}Z_{SPA-1}$ interface is inconspicuous and structure-based energetics calculations suggest that it should be capable of supporting strong binding, but that (iii) the conformational stabilization of the MG state to a well-ordered structure in the $Z{:}Z_{SPA-1}$ complex is associated with a large change in conformational entropy that opposes binding.

Introduction

Biomolecular interactions involving proteins are complex events with a number of coupled chemical processes. One level of complexity is due to the fact that they occur in water solution and in the presence cosolutes such as salts and buffer components. A second and interconnected level of complexity is conformational. The extent of conformational change in a protein upon binding a ligand is sometimes modest with only small perturbations of side chains and no changes in the protein backbone conformation. Such interactions are commonly referred to as "rigid body" interactions. Other cases which involve larger loop or domain movements or changes in secondary structure content are more loosely referred to as "induced fit" or "coupled folding". Applied fields such as protein engineering and drug discovery provide an incentive to understand the thermodynamics of binding and conformational change in detail. Unfortunately, the large body of experimental thermodynamic data that is available on protein−protein interactions (see for instance the compilation by Stites[1]) is at a first glance confounding with regard to the wide range of observed thermodynamic characteristics of protein−protein interactions; it might appear that "anything is possible". However, significant progress toward a correlation between structure and binding thermodynamics has been made in cases where conformational change is limited. The progress is due to application of empirical relations between changes in thermodynamic state functions and changes in solvent-accessible surface area[2−6] complemented with estimates of the effects of coupled folding and changes in conformational entropy.[7,8] In fact, such structure-based energetics calculations have been shown to provide almost quantitative accounting of the binding thermodynamics[9,10] in cases where high-resolution structural data on the interacting components is available and the binding does not involve for instance specific metal ion binding or polyelectrolyte effects.

Here we describe an analysis of the thermodynamics of a more complicated protein−protein interaction and support it with structure-based energetics calculations. The system consists of the Z_{SPA-1} affibody and it's Z domain binding partner. The Z domain is a small three-helix bundle protein with 58 amino acid residues derived from one of several homologous modules in staphylococcal protein A.[11] Affibodies are binding proteins obtained by combinatorial protein engineering followed by selection of a binder by panning the phage-displayed library against a target protein.[12] An affibody library contains mutant variants of the Z domain in which 13 side chains in helix I and II are randomly varied. The positions were originally selected

[†] Royal Institute of Technology (KTH).
[‡] Göteborg University.

(1) Stites, W. E. *Chem. Rev.* **1997**, *97*, 1233−1250.
(2) Murphy, K. P.; Freire, E. *Adv. Protein Chem.* **1992**, *43*, 313−361.
(3) Xie, D.; Freire, E. *Proteins: Struct., Funct., Genet.* **1994**, *19*, 291−301.
(4) Spolar, R. S.; Livingstone, J. R.; Record, M. T. *Biochemistry* **1992**, *31*, 3947−3955.
(5) Makhatadze, G. I.; Privalov, P. L. *J. Mol. Biol.* **1993**, *232*, 639−659.
(6) Privalov, P. L.; Makhatadze, G. I. *J. Mol. Biol.* **1993**, *232*, 660−679.
(7) D'Aquino, J. A.; Gomez, J.; Hilser, V. J.; Lee, K. H.; Amzel, L. M.; Freire, E. *Proteins: Struct., Funct., Genet.* **1996**, *25*, 143−156.
(8) Spolar, R. S.; Record, M. T. *Science* **1994**, *263*, 777−784.
(9) Horn, J. R.; Ramaswamy, S.; Murphy, K. P. *J. Mol. Biol.* **2003**, *331*, 497−508.
(10) Lavigne, P.; Bagu, J. R.; Boyko, R.; Willard, L.; Holmes, C. F. B.; Sykes, B. D. *Protein Sci.* **2000**, *9*, 252−264.
(11) Nilsson, B.; Moks, T.; Jansson, B.; Abrahamsén, L.; Elmblad, A.; Holmgren, E.; Henrichson, C.; Jones, T. A.; Uhlén, M. *Protein Eng.* **1987**, *1*, 107−113.
(12) Nord, K.; Gunneriusson, E.; Ringdahl, J.; Stål, S.; Uhlén, M.; Nygren, P.-Å. *Nat. Biotechnol.* **1997**, *15*, 772−777.

10.1021/ja047727y CCC: $27.50 **© 2004 American Chemical Society**

Scheme 1. Z_{SPA-1} Unfolding and Binding Equilibria

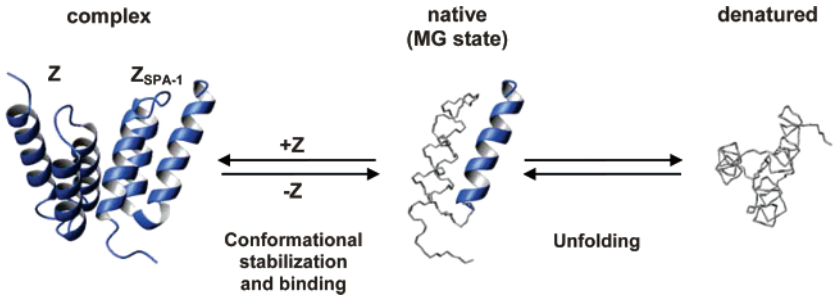

as the side chains responsible for protein interactions in the complex between the B domain of protein A and an immunoglobulin Fc domain.[13] The Z_{SPA-1} affibody was selected as a binder to protein A, and it also binds with micromolar affinity to the Z domain, i.e., its own originating scaffold.[14] Several other affibodies, some of which are high-affinity (nanomolar) binders,[15,16] have been isolated, and a range of applications has been described (see for instance refs 17 and 18). We appreciated the potential use of affibody-target protein systems as models for structural and thermodynamic studies of protein−protein interactions. With the Z:Z_{SPA-1} pair as a starting point, we determined the solution structure of the complex and carried out a preliminary characterization of Z_{SPA-1}.[19] We found that the complex contains a rather large (ca. 1600 Å^2) interaction interface with tight steric and polar/nonpolar complementarity. The structure of Z_{SPA-1} in the complex is well-ordered in a conformation that is very similar to that of the Z domain. However, the conformation of the free Z_{SPA-1} is best characterized by comparisons with protein molten globules:[20−23] it shows reduced secondary structure content, aggregation propensity, poor thermal stability, and binds the hydrophobic dye ANS.[19] This MG state of Z_{SPA-1} is the native state in the absence of the Z domain, and the ordered state is only adopted following a stabilization that occurs upon binding. A more extensive characterization of Z_{SPA-1} suggests that the average topology of the Z domain is retained in the MG state[24] but that it is represented by a multitude of rapidly interconverting conformations in which helices I and II are being transiently unfolded. Furthermore, the MG state is only marginally stable, and a significant fraction of Z_{SPA-1} exists in a completely unfolded state at room temperature.

Here we dissect the thermodynamics of the Z:Z_{SPA-1} binding equilibrium as a model for protein−protein interactions involving both a significant shift in the folding−unfolding equilibrium as well as a conformational change (stabilization) on binding. It should also be relevant for protein engineering to understand why Z_{SPA-1} is an intermediate-affinity (μM) and not a high-affinity (nM) binding protein; that is, to investigate if suboptimal binding is primarily due to the structure of the binding surface or to the fact that Z_{SPA-1} is forced to adopt an ordered structure or if it simply can be attributed to the poor thermal stability of the MG state. The analysis is based in Scheme 1, which shows the thermodynamic states and equilibria that are relevant at low (μM) Z_{SPA-1} concentrations. The available structural information consists of the structure of the free Z domain, determined in solution using NMR,[25] the structure of the Z:Z_{SPA-1} complex, which was determined using both NMR[19,26] and X-ray crystallography,[27] and the fact that the MG state of Z_{SPA-1} has been characterized to the extent that the average secondary structure content and topology are known,[24] as described above.

The strategy is to first analyze the thermodynamics of thermal unfolding of both Z and Z_{SPA-1}. These data yield the temperature-dependent equilibrium constant for unfolding of the MG state of Z_{SPA-1} (K_{unfold}) and the unfolding enthalpy ($\Delta H°_{unfold}$). The unfolding thermodynamics is then used to subtract the effect of MG state folding from the effect of stabilization and binding in ITC (isothermal titration calorimetry) data on the Z:Z_{SPA-1} equilibrium. The deconvoluted binding thermodynamics obtained in this way can be viewed as containing contributions for the transition from an MG state of Z_{SPA-1} to the well-ordered structure found in the complex (conformational stabilization) *and* the thermodynamic contributions for binding of such a stabilized Z_{SPA-1} structure to the Z domain. It is not possible to experimentally separate the processes of stabilization and binding. It is, however, possible to compare the observed binding thermodynamics to what would be expected from a *hypothetical* binding reaction in which Z (free state structure known) and Z_{SPA-1} (ordered three-helix bundle structure assumed) form a Z:Z_{SPA-1} complex (structure known). This comparison then yields clues with regard to the thermodynamic contribution from the conformational stabilization of Z_{SPA-1} upon complex formation. Independent analyses of the binding entropy and the expected effects based on (known) changes in secondary structure content then, finally, confirm unfavorable and favorable contributions to binding arising from changes in conformational entropy and desolvation effects, respectively. The analysis also provides a comparison of the thermal stability of the Z_{SPA-1}

(13) Deisenhofer, J. *Biochemistry* **1981**, *20*, 2361−2370.
(14) Eklund, M.; Axelsson, L.; Uhlén, M.; Nygren, P.-Å. *Proteins: Struct., Funct., Genet.* **2002**, *48*, 454−462.
(15) Nord, K.; Nord, O.; Uhlén, M.; Kelley, B.; Ljungqvist, C.; Nygren, P.-Å. *Eur. J. Biochem.* **2001**, *268*, 4269−4277.
(16) Gunneriusson, E.; Nord, K.; Uhlén, M.; Nygren, P.-Å. *Protein Eng.* **1999**, *12*, 873−878.
(17) Rönnmark, J.; Hansson, M.; Nguyen, T.; Uhlén, M.; Robert, A.; Ståhl, S.; Nygren, P.-Å. *J. Immunol. Methods* **2002**, *261*, 199−211.
(18) Gunneriusson, E.; Samuelson, P.; Ringdahl, J.; Grönlund, H.; Nygren, P.-Å.; Ståhl, S. *Appl. Environ. Microbiol.* **1999**, *65*, 4134−4140.
(19) Wahlberg, E.; Lendel, C.; Helgstrand, M.; Allard, P.; Dincbas-Renqvist, V.; Hedqvist, A.; Berglund, H.; Nygren, P.-Å.; Härd, T. *Proc. Natl. Acad. Sci. U.S.A.* **2003**, *100*, 3185−3190.
(20) Semisotnov, G.; Rodionova, N.; Razgulyaev, O.; Uversky, V.; Gripas, A.; Gilmanshin, R. *Biopolymers* **1991**, *31*, 119−128.
(21) Dobson, C. *Curr. Biol.* **1994**, *4*, 636−640.
(22) Ptitsyn, O. *Trends Biochem. Sci.* **1995**, *20*, 376−379.
(23) Regan, L. *Proc. Natl. Acad. Sci. U.S.A.* **2003**, *100*, 3553−3554.
(24) Lendel, C.; Dincbas-Renqvist, V.; Flores, A.; Wahlberg, E.; Dogan, J.; Nygren, P.-Å.; Härd, T. *Protein Sci.* **2004**, *13*, 2078−2088.
(25) Zheng, D.; Aramini, J. M.; Montelione, G. T. *Protein Sci.* **2004**, *13*, 549−554.
(26) Lendel, C.; Wahlberg, E.; Berglund, H.; Eklund, M.; Nygren, P.-Å.; Härd, T. *J. Biomol. NMR* **2002**, *24*, 271−272.
(27) Högbom, M.; Eklund, M.; Nygren, P.-Å.; Nordlund, P. *Proc. Natl. Acad. Sci. U.S.A.* **2003**, *100*, 3191−3196.

affibody as compared to the originating Z domain including a measure of the heat capacity change ($\Delta C_P°$) for the formation of the MG state from the completely unfolded state, which provides an additional illustration of the conformational dynamics of a molten-globule-like protein.

Methods

Proteins and Chemicals. The Z domain and the Z_{SPA-1} affibody were produced and purified as described previously.[26] Concentrations were determined spectrophotometrically using values for the extinction coefficients $\epsilon_{280} = 5500\ M^{-1}\ cm^{-1}$ for Z_{SPA-1} and $\epsilon_{275} = 1490\ M^{-1}\ cm^{-1}$ for Z calculated for tryptophan and tyrosine absorption. TMAO (trimethylamine *N*-oxide dihydrate; 98% purity), betaine ((carboxymethyl)trimethylammonium hydroxide; inner salt; anhydrous; 98% purity), and analytical grade guanidine hydrochloride (GuaHCl) were obtained from Sigma-Aldrich.

CD Measurements of Helix Content and Thermal Unfolding. The thermal denaturation of Z_{SPA-1} and Z was monitored by circular dichroism (CD) using a Jasco J-810 spectropolarimeter with a Peltier type temperature controller (Jasco PTC-423S) and a cell with an optical path length of 1 cm. The samples contained 20 to 25 μM protein in 20 mM potassium phosphate buffer at pH 5.7 or 7.25, with or without 1 M TMAO (Z_{SPA-1}), or at pH 5.7 with 0, 1, or 2 M GuaHCl (Z domain). The CD signal (ellipticity) was measured at 222 nm as a function of temperature and converted to molar ellipticity prior to analysis. Heating rates of 120 °C h^{-1} or 30 °C h^{-1} with a detection response time of 2 s were used. No significant differences could be detected between data sets obtained with these two heating rates.

The fraction helix f_H was calculated from the molar ellipticity at 222 nm according to

$$f_H = \frac{([\theta]_{obsd} - [\theta]_C)}{([\theta]_H - [\theta]_C)} \quad (1)$$

where $[\theta]_{obsd}$ is the observed molar ellipticity, and the reference values $[\theta]_H$ and $[\theta]_C$ for 100% α-helix or 100% random coil, respectively, are given by[28]

$$[\theta]_H = -40000\left(1 - \frac{2.5}{n}\right) + 100T \quad (2)$$

$$[\theta]_C = 640 - 45T \quad (3)$$

in which T is the temperature in °C and $n = 58$ is the number of amino acid residues in Z and Z_{SPA-1}.

van't Hoff Analysis of Thermal Stability. Thermal melting profiles of Z_{SPA-1} and Z were analyzed using a two-state model for the unfolding thermodynamics. The molar ellipticity is then

$$[\theta]_{obsd} = (1 - f_{unfold})[\theta]_N + f_{unfold}[\theta]_U \quad (4)$$

in which $[\theta]_N$ and $[\theta]_U$ represent temperature-dependent molar ellipticities of the native and unfolded states, respectively. The fraction of unfolded protein f_{unfold} is related to the equilibrium unfolding constant K_{unfold} as

$$f_{unfold} = \frac{K_{unfold}}{K_{unfold} + 1} \quad (5)$$

The thermodynamics that determine K_{unfold} is given by

$$K_{unfold} = \exp\left(\frac{-\Delta G°_{unfold}}{RT}\right) = \exp\left(\left(\frac{-1}{RT}\right)\left(\Delta H°_{unfold,ref} - T\Delta S°_{unfold,ref} + \Delta C°_{P,unfold}\left(T - T_{ref} - T\ln\frac{T}{T_{ref}}\right)\right)\right) \quad (6)$$

in which R is the gas constant, $\Delta G°_{unfold}$ is the free energy difference between native and unfolded states, and $\Delta H°_{unfold,ref}$ and $\Delta S°_{unfold,ref}$ are enthalpy and entropy differences, respectively, at the reference temperature T_{ref} (here chosen to be 25 °C). The heat capacity change $\Delta C_{P,unfold}$ has been assumed to be temperature independent. [The subscript $_{unfold}$ has been introduced to distinguish the folding thermodynamics from the binding thermodynamics.] An alternative parametrization of the free energy difference can be made to obtain

$$K_{unfold} = \exp\left(\frac{-\Delta G°_{unfold}}{RT}\right) = \exp\left(\left(\frac{-1}{RT}\right)\left(\Delta C°_{P,unfold}\left(T - T_H - T\ln\frac{T}{T_s}\right)\right)\right) \quad (7)$$

where two references temperatures T_H and T_S are defined by $\Delta H°_{unfold}(T_H) = 0$ and $\Delta S°_{unfold}(T_S) = 0$.

Equations 4 and 5, together with either eq 6 or 7, were fitted to experimental data using nonlinear least-squares regression routines available within Origin 7.0 (OriginLab Corporation, 2002). The molar ellipticities of the native and unfolded states were assumed to be linear functions of temperature;[28] $[\theta]_N = a_N + b_N T$ and $[\theta]_U = a_U + b_U T$. The values of the four a_N, b_N, a_U, and b_U coefficients were determined by fitting data at the low and high-temperature ends of the melting profiles or by optimization together with the thermodynamics parameters. The possibility that $\Delta C°_{P,unfold}$ in eq 6 is insignificantly small was tested by comparing the F-statistics[29] for fits with a fixed value $\Delta C°_{P,unfold} = 0$ to fits in which $\Delta C°_{P,unfold}$ was an adjustable parameter. To assess the quality of the data and the fits, we compared results obtained with eq 6 to those obtained with eq 7 by interconverting values of T_H and T_S to values of $\Delta H°_{unfold}$ and $\Delta S°_{unfold}$ at 25 °C and *vice versa* (Table 1). Other parameters such as the melting temperature T_m for which $\Delta G°_{unfold}(T_m) = 0$ can be calculated from any set of fitted parameters using standard thermodynamic relationships. Standard errors in best-fit values were calculated from the covariance matrix, and these errors were propagated to other parameters derived from best-fit values.

ITC Analysis of the Z:Z_{SPA-1} Binding Equilibrium. The thermodynamics of Z:Z_{SPA-1} association was measured using a MCS-ITC titration microcalorimeter (MicroCal Inc., Northampton, MA) with a cell volume of 1.3608 mL. All solutions were degassed before the ITC experiments, which were performed at different temperatures in 20 mM potassium phosphate buffer at pH 5.7 and 7.25 with or without added TMAO or betaine and at 25 °C in 20 mM Tris buffer at pH 7.25. The protein samples were dialyzed against the same batch of buffer prior to experiments to minimize artifacts due to minor differences in buffer composition. Solutions of Z at concentrations in the range 300 to 400 μM were injected into the calorimeter cell containing 30 to 40 μM of Z_{SPA-1}. A typical experiment consisted of a 2 μl preliminary injection followed by 24 subsequent 10 μl injections. Reaction heats observed toward the end of the titrations were similar to the heats of dilution measured in control experiments where Z was titrated into buffer. Baseline correction and integration of the calorimeter response was carried out using the Origin software (MicroCal Inc.) provided with the calorimeter. The obtained binding enthalpy values were then corrected for heats of dilution and fitted to a model in which the variable parameters are the stoichiometry of identical sites (n), an apparent dissociation constant (K_d^{app}), and an apparent association enthalpy (ΔH_{ITC}). We note that all thermodynamic quantities reported here are calculated based on macromolecular concentrations and neglecting any nonideality of the solutions. They are therefore only relevant at specific buffer and concentration conditions.

Deconvolution of Folding and Binding Thermodynamics. The calorimetrically measured enthalpy of binding of Z_{SPA-1} to the Z

(28) Scholtz, J. M.; Quian, H.; York, E. J.; Stewart, J. M.; Baldwin, R. L. *Biopolymers* **1991**, *31*, 1463−1470.
(29) Devore, J. L. *Probability and statistics for engineering and the sciences*; 4th Ed. ed.; Wadsworth, Inc./International Thomson Publishing Inc.: USA, 1995.

Table 1. Thermodynamics for Z_{SPA-1} and Z Domain Unfolding at 25 °C[a]

protein/conditions	equation	ΔH°_{unfold} kcal mol^{-1}	$\Delta C^\circ_{P,unfold}$ cal mol^{-1} K^{-1}	ΔS°_{unfold} cal mol^{-1} K^{-1}	ΔG°_{unfold} kcal mol^{-1}	T_m (°C)	T_S (°C)	T_H (°C)
				Z_{SPA-1}				
pH 7.25	6	**30.3 ± 0.1**	**0 (fixed)**	**96 ± 0.3**	1.7 ± 0.2	42.4 ± 1.4	*c*	*c*
		30.1 ± 0.4	**−39 ± 114**	**96 ± 1**	1.5[b]	40.5[b]	*d*	*d*
	7	28 ± 5	**97 ± 16**	88 ± 15	1.4[b]	40.0[b]	**−153 ± 3**	**−260 ± 6**
pH 7.25, 1 M TMAO	6	**30.1 ± 0.1**	**0 (fixed)**	**94 ± 0.3**	2.1 ± 0.2	47.0 ± 1.5	*c*	*c*
		29.9 ± 0.9	**122 ± 195**	**92 ± 2**	2.5[b]	50.4[b]	*d*	*d*
	7	30 ± 5	**105 ± 16**	94 ± 14	2.3[b]	49.6	**−151 ± 2**	**−264 ± 6**
pH 5.7	6	**30.8 ± 0.1**	**0 (fixed)**	**98 ± 0.3**	1.6 ± 0.2	41.1 ± 1.4	*c*	*c*
		30.0 ± 0.4	**27 ± 198**	**96 ± 1**	1.4[b]	39.2[b]	*d*	*d*
	7	28 ± 5	**100 ± 18**	90 ± 16	1.5[b]	40.7	**−152 ± 3**	**−258 ± 7**
pH 5.7, 1 M TMAO	6	**30.2 ± 0.1**	**0 (fixed)**	**93 ± 0.3**	2.5 ± 0.2	51.5 ± 1.5	*c*	*c*
		30.2 ± 0.7	**160 ± 147**	**93 ± 2**	2.5[b]	49.8[b]	*d*	*d*
	7	32 ± 5	**110 ± 16**	98 ± 14	2.6[b]	49.6	**−151 ± 2**	**−264 ± 5**
				Z domain				
pH 5.7	6	**21.0 ± 1.5**	**415 ± 62**	**54 ± 3**	4.9 ± 2.4	79.5[b]	−11 ± 8	−26 ± 5
	7	26 ± 4	**300 ± 43**	71 ± 11	5.2[b]	78.5[b]	**−38 ± 4**	**−63 ± 5**
pH 5.7, 1 M GuaHCl	6	**27.3 ± 0.9**	**335 ± 104**	**78 ± 2**	4.1 ± 1.5	65.5[b]	−37 ± 25	−56 ± 17
	7	27 ± 4	**335 ± 46**	78 ± 11	4.2[b]	66.7[b]	**−37 ± 2**	**−57 ± 7**
pH 5.7, 2 M GuaHCl	6	**26.7 ± 1.3**	**316 ± 209**	**80 ± 3**	2.9 ± 2.2	54.8[b]	-42 ± 56	−59 ± 38
	7	27 ± 7	**390 ± 107**	73 ± 21	2.7[b]	54.9[b]	**−26 ± 4**	**−38 ± 6**

[a] Numbers in bold are best-fit values. Other numbers are derived from best-fit values. [b] Errors not determined due to co-variation of errors in other parameters. [c] T_S and T_H not defined when $\Delta C^\circ_{P,unfold} = 0$. [d] Not determined due to uncertainty in $\Delta C^\circ_{P,unfold}$.

domain, ΔH_{ITC}, contains contributions from the intrinsic binding event, ΔH°_{bind}, and the enthalpy of folding of the fraction f_{unfold} of Z_{SPA-1} that is unfolded in the absence of Z. Hence, corrected binding enthalpies were obtained using

$$\Delta H^\circ_{bind} = \Delta H_{ITC} - f_{unfold}\Delta H^\circ_{fold} = \Delta H_{ITC} + f_{unfold}\Delta H^\circ_{unfold} \quad (8)$$

where f_{unfold} and ΔH°_{bind} were obtained from the van't Hoff analysis of the thermal stability of Z_{SPA-1} as described above. The corrected ΔH°_{bind} values at different temperatures were fitted to

$$\Delta H^\circ_{bind}(T) = \Delta H^\circ_{bind,ref} + \Delta C^\circ_{P,bind}(T - T_{ref}) \quad (9)$$

to obtain the best-fit values of ΔH°_{bind} at $T_{ref} = 25$ °C and $\Delta C^\circ_{P,bind}$.

The apparent dissociation constant for the Z_{SPA-1}:Z complex measured by ITC (K_d^{app}) contains contributions from the actual binding reaction (dissociation constant K_d) as well as from folding of Z_{SPA-1}. Considering the linked equilibria in Scheme 1, one can derive

$$K_d = \frac{K_d^{app}}{1 + K_{unfold}} \quad (10)$$

from which the free energy for the binding reaction ΔG°_{bind} can be obtained as

$$\Delta G^\circ_{bind} = -RT\ln\left(\frac{1}{K_d}\right) = -RT\ln\left(\frac{1 + K_{unfold}}{K_d^{app}}\right) \quad (11)$$

Corrected K_d values were calculated for the ITC experiments (Table 2), and values at different temperatures were fitted to an expression completely analogous to eq 6 to obtain $\Delta S^\circ_{bind,ref}$. (The best-fit values of $\Delta H^\circ_{bind,ref}$ and $\Delta C^\circ_{P,bind}$ to eq 9 were treated as fixed parameters in these fits.)

Structure-Based Calculations of Thermodynamic Parameters. Calculations of binding thermodynamics were performed using the parametrization of ΔC°_P, ΔH°, and ΔS° in terms of changes in accessible surface area (ΔASA) and experimentally calibrated conformational entropy effects derived by Freire, Murphy, and collaborators.[2,3,7,30] This parametrization was obtained from protein unfolding data, but it is equally applicable to protein binding.[31] We used the implementation of the methodology that is available as the STC (structure-based thermodynamics calculation) suite of programs (ref 10, available at http://www.pence.ca/ftp/). All methods and parameters including calculation of surface areas (1.4Å probe) and parametrization of ΔC°_P and ΔH° were those described by Lavigne et al..[10]

For later reference we explain the treatment of the dissociation entropy term in more detail. It is divided into contributions from changes in solvation (ΔS_{solv}), conformational entropy (ΔS_{conf}), and rotational and translational entropy (ΔS_{rt}):

$$\Delta S^\circ(T) = \Delta S_{solv}(T) + \Delta S_{conf} + \Delta S_{rt} \quad (12)$$

in which the solvation term is calculated from ΔASA values[7]

$$\Delta S_{solv}(T) = 0.45\Delta ASA_{np}\ln(T/384) - 0.26\Delta ASA_p\ln(T/335) \quad (13)$$

The appropriate value for the change in rotational and translational entropy is a matter of some discussion. We use the cratic entropy value $\Delta S_{rt} = R\ln(1/55) = -8$ cal mol^{-1} K^{-1}, corresponding to $-T\Delta S_{rt} = 2.4$ kcal mol^{-1} at 25 °C, which is numerically close to values suggested by recent experimental and theoretical work.[32,33] The contribution to conformational entropy is further divided as (see ref 7 and work cited therein)

$$\Delta S_{conf} = \Delta S_{bu\to ex} + \Delta S_{ex\to u} + \Delta S_{bb} \quad (14)$$

in which $\Delta S_{bu\to ex}$ is due to the increase in entropy of a side chain when it is moved from a buried to exposed environment, $\Delta S_{ex\to u}$ represents the side chain entropy gained when a secondary structure unfolds, and ΔS_{bb} is the corresponding gain in backbone entropy on unfolding. Values for these entities (which in general are positive for unfolding and negative for folding) have been measured for all side chains except proline.[7,34] Here, we set $\Delta S_{ex\to u} = \Delta S_{bb} = 0$ in the calculations and treat $\Delta S_{bu\to ex}$ as in ref 10 in the calculations on the reaction with hypothetically stabilized Z_{SPA-1}. We also make use of tabulated values

(30) Hilser, V. J.; Gomez, J.; Freire, E. *Proteins: Struct., Funct., Genet.* **1996**, *26*, 123−133.
(31) Gomez, J.; Freire, E. *J. Mol. Biol.* **1995**, *252*, 337−350.
(32) Yu, Y.; Lavigne, P.; Kay, C. M.; Hodges, R. S.; Privalov, P. L. *J. Phys. Chem. B* **1998**, *103*, 2270−2278.
(33) Amzel, L. *Proteins: Struct., Funct., Genet.* **1997**, *28*, 144−149.
(34) Lee, K. H.; Xie, D.; Freire, E.; Amzel, L. M. *Proteins: Struct., Funct., Genet.* **1994**, *20*, 68−84.

Table 2. Isothermal Titration Calorimetry Data for Z:Z_{SPA-1} Association

		values from ITC			corrected for folding[a]		
conditions	temp (°C)	ΔH_{ITC} (kcal mol^{-1})	K_d^{app} (μM)	n	f_{unfold}	ΔH°_{bind} (kcal mol^{-1})	K_d (μM)
pH 7.25	10.8	−0.3 ± 0.1	1.5 ± 1.0	1.15 ± 0.04	0.005	−0.2 ± 0.1	1.5 ± 1.0
	12.9	−1.2 ± 0.1	1.3 ± 0.6	0.97 ± 0.02	0.007	−1.0 ± 0.1	1.3 ± 0.6
	14.8	−2.4 ± 0.1	1.6 ± 0.7	0.98 ± 0.03	0.010	−2.1 ± 0.1	1.6 ± 0.7
	16.8	−2.5 ± 0.1	0.52 ± 0.2	1.01 ± 0.01	0.014	−2.1 ± 0.1	0.52 ± 0.2
	18.8	−3.5 ± 0.1	0.61 ± 0.1	0.93 ± 0.01	0.020	−2.9 ± 0.1	0.59 ± 0.1
	21.5	−4.7 ± 0.1	0.81 ± 0.1	1.09 ± 0.01	0.031	−3.7 ± 0.1	0.79 ± 0.1
	24.1	−7.2 ± 0.1	0.79 ± 0.1	0.92 ± 0.01	0.049	−5.7 ± 0.1	0.75 ± 0.1
	27.1	−8.7 ± 0.1	0.97 ± 0.1	1.01 ± 0.01	0.078	−6.3 ± 0.1	0.90 ± 0.1
	30.2	−11.0 ± 0.1	1.0 ± 0.1	0.92 ± 0.01	0.125	−7.3 ± 0.1	0.89 ± 0.1
pH 7.25, 20 mM Tris	25.2	−9.5 ± 0.1	0.61 ± 0.1	0.96 ± 0.01			
pH 5.7	12.5	−2.3 ± 0.1	3.4 ± 1.1	0.86 ± 0.02	0.008	−2.1 ± 0.1	3.4 ± 1.1
	14.4	−3.0 ± 0.1	1.9 ± 0.3	0.84 ± 0.01	0.012	−2.6 ± 0.1	1.9 ± 0.3
	15.7	−3.6 ± 0.1	0.95 ± 0.3	0.89 ± 0.02	0.015	−3.2 ± 0.1	0.94 ± 0.3
	18.1	−4.8 ± 0.1	0.79 ± 0.3	0.89 ± 0.02	0.023	−4.1 ± 0.1	0.78 ± 0.3
	21.2	−5.7 ± 0.1	1.6 ± 0.1	0.81 ± 0.01	0.039	−4.5 ± 0.1	1.5 ± 0.1
	24.1	−7.7 ± 0.1	2.0 ± 0.3	0.80 ± 0.01	0.065	−5.6 ± 0.1	1.9 ± 0.3
	27.1	−11.4 ± 0.1	1.8 ± 0.2	0.91 ± 0.01	0.105	−8.1 ± 0.1	1.6 ± 0.2
	30.1	−13.9 ± 0.2	1.7 ± 0.3	0.90 ± 0.01	0.163	−8.9 ± 0.2	1.4 ± 0.3
pH 7.25, 1 M TMAO	13.7	−2.1 ± 0.1	0.6 ± 0.15	0.96 ± 0.01	0.002	−2.0 ± 0.1	0.6 ± 0.15
	15.3	−2.8 ± 0.1	0.5 ± 0.15	1.04 ± 0.01	0.003	−2.7 ± 0.1	0.5 ± 0.15
	20.0	−4.1 ± 0.1	0.25 ± 0.05	0.96 ± 0.01	0.008	−3.8 ± 0.1	0.25 ± 0.05
	25.0	−6.3 ± 0.1	0.37 ± 0.05	0.91 ± 0.01	0.018	−5.8 ± 0.1	0.36 ± 0.05
	30.1	−8.2 ± 0.1	0.51 ± 0.06	0.99 ± 0.01	0.041	−7.0 ± 0.1	0.49 ± 0.06
pH 7.25, 3 M betaine	13.2	1.0 ± 0.1	0.4 ± 0.2	0.88 ± 0.02			
	20.6	−1.7 ± 0.1	1.3 ± 0.7	0.81 ± 0.03			
	24.1	−3.0 ± 0.1	1.0 ± 0.2	1.07 ± 0.01			
	30.1	−5.5 ± 0.1	1.5 ± 0.2	0.91 ± 0.01			

[a] Z:Z_{SPA-1} binding parameters corrected for the shift in the equilibrium between the MG and completely unfolded states of Z_{SPA-1}. ITC data for betaine containing samples could not be corrected due to reasons described in the text.

for $\Delta S_{ex\rightarrow u}$ and ΔS_{bb} (ref 7) when estimating loss of conformational entropy for the actual stabilization of Z_{SPA-1}.

Results

Z and Z_{SPA-1} Folding Thermodynamics. The thermal stability of Z_{SPA-1} was monitored at pH 5.7 and 7.25 in the presence and absence of 1 M TMAO. The stability of the Z domain was measured at pH 5.7 in the presence of 0, 1, and 2 M GuaHCl. Examples of melting profiles are shown in Figure 1. Z_{SPA-1} is significantly less stable than the Z domain and has a T_m value of 42 °C, compared to 79 °C for Z. There is no significant difference between Z_{SPA-1} stabilities measured at pH 5.7 and 7.25, but the addition of 1 M TMAO is stabilizing and the T_m value increases to approximately 50 °C. The Z domain is destabilized by the addition of GuaHCl, as expected.

The thermodynamics of unfolding was quantified using eqs 6 and 7 (Table 2). The fitting procedure involves simultaneous optimization of six or seven parameters. It is nevertheless restrained if the ellipticity baselines for the native and unfolded states are sufficiently long. This is the case for Z_{SPA-1} in the presence of TMAO and for Z in the presence of GuaHCl. Comparisons between best-fit thermodynamic parameters obtained in the presence and absence of cosolvent or at different pH values can then give an indication of the reliability of the thermodynamic data in the absence of TMAO or GuaHCl, also when the pre- and postmelting baselines are less well-defined.

Fits to eq 6 show that thermal unfolding of Z_{SPA-1} occurs with an enthalpy change on the order of 30 kcal mol^{-1} and entropy changes in the range 96−98 and 92−93 cal mol^{-1} K^{-1} in the absence and presence of TMAO, respectively. The fits are very good also when the heat capacity change is fixed to $\Delta C^\circ_{P,unfold} = 0$ (Figure 1). Attempts to resolve a small value of $\Delta C^\circ_{P,unfold}$ in eq 6 by allowing it to vary were not successful because the inclusion of the extra variable parameter was not statistically significant. Fitting the melting data to eq 7, which relies on obtaining a more precise value of $\Delta C^\circ_{P,unfold}$ on expense of the precision of other parameters, yields values around 100 cal mol^{-1} K^{-1}. We conclude that Z_{SPA-1} unfolding involves a heat capacity change which is small but that a precise value, possibly in the range 0 to 200 cal mol^{-1} K^{-1}, cannot be resolved using thermal melting experiments. The stabilizing effect of TMAO on Z_{SPA-1} is due to a subtle effect on the unfolding entropy, whereas the enthalpy change is unaffected within the resolution of our experiments.

With the Z domain, we find that it is not possible to fit $\Delta H^\circ_{unfold,ref}$ and $\Delta S^\circ_{unfold,ref}$ in eq 6 when the heat capacity change is fixed to $\Delta C^\circ_{P,unfold} = 0$ (Figure 1). Simultaneous optimization of all three parameters yield ΔH°_{unfold} values in the range 21 to 27 kcal mol^{-1} K^{-1} and ΔS°_{unfold} values in the range 50 to 80 cal mol^{-1} K^{-1} (25 °C) depending on GuaHCl concentration. Best-fit values of $\Delta C^\circ_{P,unfold}$ consistently fall within the range 300 to 400 cal mol^{-1} K^{-1} at the different GuaHCl concentrations and when using different parametrization of the free energy. (An effect of denaturant on protein unfolding heat capacity is not expected.[35]) We conclude that the Z domain unfolds with a smaller ΔH°_{unfold} than Z_{SPA-1} and that the thermal stability difference between the two proteins is due to entropic effects in combination with a significantly larger heat capacity change upon folding of the Z domain. The effect of denaturant on the thermodynamics of Z unfolding appears to be a combination of enthalpic and entropic effects, but the

(35) Felitsky, D. J.; Record, M. T. *Biochemistry* **2003**, *42*, 2202−2217.

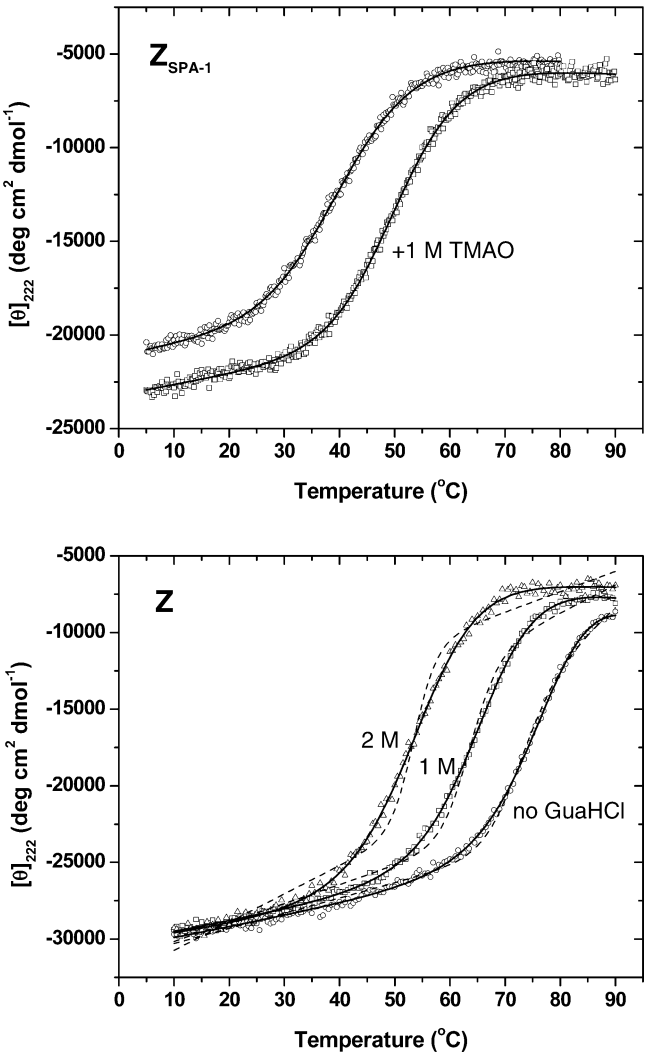

Figure 1. Thermal denaturation of Z_{SPA-1} and Z at pH 5.7 monitored as molar ellipticity at 222 nm. Solid lines with the Z_{SPA-1} data represent fits to eq 6 with $\Delta C^\circ_{P,unfold} = 0$ (fixed). With the Z data, solid lines represent fits to eq 6 with $\Delta C^\circ_{P,unfold}$ treated as an adjustable parameter and dashed lines fit with $\Delta C^\circ_{P,unfold} = 0$ (fixed).

evidence is inconclusive because of the uncertainties associated with the thermal melting data of Z in absence of GuaHCl.

Thermodynamics of Z:Z_{SPA-1} Complex Formation. The Z:Z_{SPA-1} binding equilibrium was monitored using ITC in the temperature range 10 to 30 °C and at four buffer conditions: phosphate buffer at pH 7.25 and 5.7, and at pH 7.25 in the presence of 1 M TMAO or 3 M betaine. Additional experiments in Tris buffer were also performed in order to investigate any protonation effects. The osmolytes TMAO and betaine were used to monitor binding of the fully formed MG state Z_{SPA-1} to validate the procedure used to deconvolute the binding thermodynamics from effects arising from the MG state-to-unfolded equilibrium. An example of the ITC data is shown in Figure 2, and the analyses of all experiments are summarized in Table 2. Complex formation is found to be an exothermic reaction at all temperatures except with 3 M betaine at low temperatures. The apparent dissociation constants are 0.6 to 3 μM in buffer and 0.25 to 0.6 μM (stronger binding) in the presence of 1 M TMAO. The reaction enthalpies are linear functions of temperature in the presence of TMAO and betaine but significantly nonlinear in the absence of osmolytes, as shown

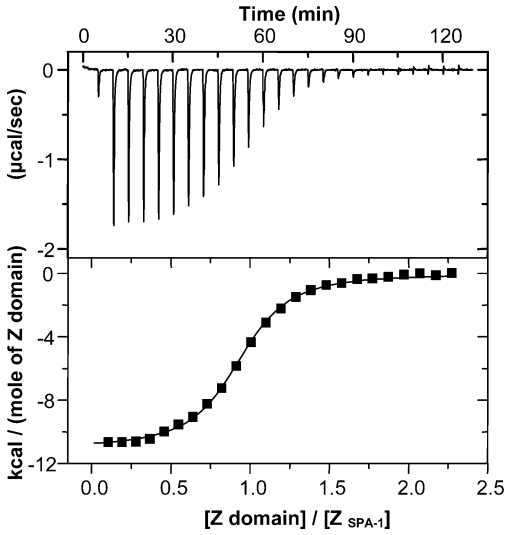

Figure 2. Isothermal titration calorimetry (ITC) data for titration of the Z domain onto the Z_{SPA-1} affibody at 30 °C in 20 mM potassium phosphate buffer at pH 7.25. The upper panel shows the baseline corrected instrumental response. The lower panel shows the integrated data (solid squares) and the best-fit of the binding parameters (solid line).

in Figure 3. We attribute the nonlinearity to a temperature-dependent shift of the folded−unfolded equilibrium of MG state Z_{SPA-1} which is coupled to the stabilization and binding of Z_{SPA-1} to Z.

The thermal stability parameters determined in the previous section predict that 13% (pH 7.25) and 16% (pH 5.7) of Z_{SPA-1} is unfolded at 30 °C and in the absence of the Z domain, whereas the corresponding fraction at pH 7.25 and 1 M TMAO is 4%. The apparent binding enthalpies were therefore corrected for the effects expected for Z_{SPA-1} folding, and the results are shown in Figure 3 and Table 2. As an example, the apparent binding enthalpy at 30 °C and pH 5.7 is −13.9 kcal mol^{-1}, but this value becomes −8.9 kcal mol^{-1} when the exothermic heat of folding of 16.3% of Z_{SPA-1} with a folding enthalpy of −30.1 kcal mol^{-1} has been subtracted.

The corrected binding enthalpies show linear temperature dependencies (Figure 3) and were thus fitted to eq 9 to obtain values of $\Delta C^\circ_{P,bind}$ and ΔH°_{bind} at 25 °C. The apparent binding constants were also corrected using eq 10 (Table 2), but these corrections are less dramatic and always less than 20%. The resulting K_d values were translated to ΔG°_{bind} at different temperatures (not shown), and these data were used together with the previously determined $\Delta C^\circ_{P,bind}$ and ΔH°_{bind} to obtain the reference values of ΔS°_{bind} and, subsequently, a reference value for ΔG°_{bind} at 25 °C. The ITC data obtained in the presence of betaine could not be corrected for folding effects, because the strong absorption in the far-UV region prohibits CD and stability measurements of Z_{SPA-1} in betaine containing solutions. However, the effect of 3 M betaine on the NMR spectrum of Z_{SPA-1} is very similar to that of 1 M TMAO (not shown) suggesting that the two osmolytes have similar effects on Z_{SPA-1} stability and that the required corrections therefore are small.

The thermodynamic parameters for the Z:Z_{SPA-1} binding equilibrium are summarized in Table 3. This table also contains the values of the temperatures T_H (above which association has a favorable enthalpy contribution), and T_S (below which association is favored by entropy effects; T_H and T_S are also

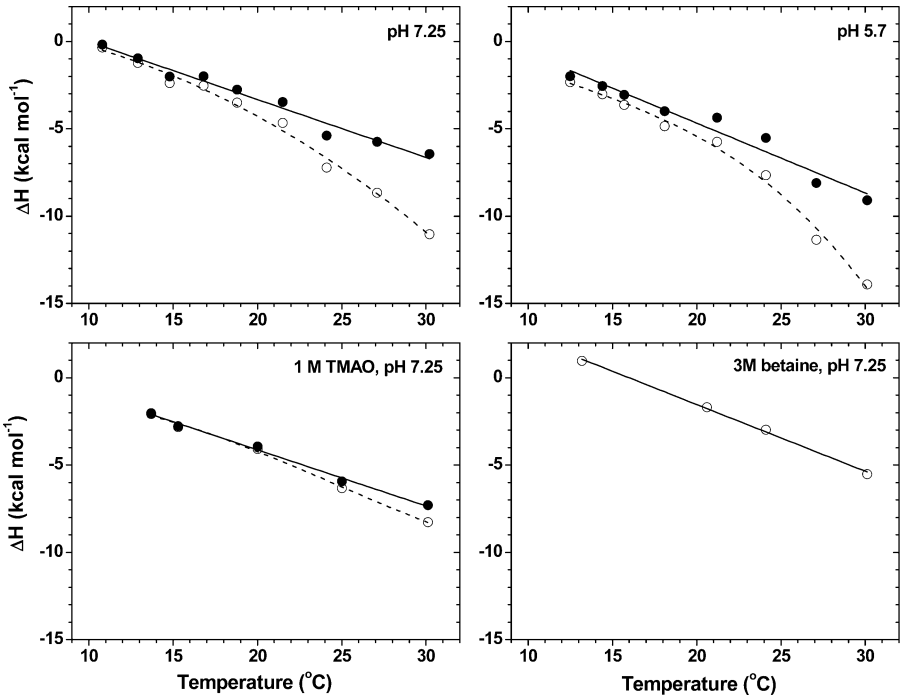

Figure 3. Observed binding enthalpies for Z:Z_{SPA-1} complex formation (○) and enthalpies corrected for Z_{SPA-1} folding (●). All data refer to measurements in 20 mM phosphate buffer at pH and cosolute conditions as indicated in the different panels. The solid lines are linear fits to determine $\Delta C^{\circ}_{P,bind}$ and ΔH°_{bind}. Dashed lines are cubic fits to uncorrected data.

Table 3. Thermodynamics of the Z:Z_{SPA-1} Interaction at 25 °C Corrected for Z_{SPA-1} Folding[a]

conditions	$\Delta C^{\circ}_{P,bind}$ cal mol^{-1} K^{-1}	ΔH°_{bind} kcal mol^{-1}	ΔS°_{bind} cal mol^{-1} K^{-1}	$-T\Delta S^{\circ}_{bind}$ kcal mol^{-1}	ΔG°_{bind} kcal mol^{-1}	K_d° (μM)	T_S (°C)	T_H (°C)	$K_d(T_H)$ (μM)
pH 7.25	-370 ± 20	-5.5 ± 0.2	9.1 ± 0.3	-2.7 ± 0.1	-8.2 ± 0.3	1.0 ± 0.6	32 ± 1	10 ± 1	0.7 ± 0.4
pH 5.7	-400 ± 30	-6.8 ± 0.2	3.7 ± 0.3	-1.1 ± 0.1	-7.9 ± 0.3	1.6 ± 0.3	28 ± 1	8 ± 2	0.9 ± 0.5
pH 7.25, 1 M TMAO	-310 ± 10	-5.5 ± 0.1	10.4 ± 0.4	-3.1 ± 0.1	-8.6 ± 0.2	0.5 ± 0.2	35 ± 1	7 ± 1	0.3 ± 0.1
pH 7.25, 3 M betaine[a]	-390 ± 10	-3.5 ± 0.1	16.2 ± 0.5	-4.8 ± 0.2	-8.3 ± 0.3	0.8 ± 0.4	38 ± 1	16 ± 0.5	0.6 ± 0.4

[a] Data obtained with 3 M betaine are not corrected (see text).

the temperatures for optimum binding affinity and minimum in ΔG°_{bind}, respectively). Complex formation at 25 °C is in all cases favored by both entropy and enthalpy changes, but the values of ΔH°_{bind} and $-T\Delta S^{\circ}_{bind}$ vary with 0 to 3 kcal mol^{-1} between the different solution conditions.

The differences observed between pH 5.7 ($\Delta H^{\circ}_{bind} = -6.8$ kcal mol^{-1}) and 7.25 ($\Delta H^{\circ}_{bind} = -5.5$ kcal mol^{-1}) could be due to a protonation linkage effect,[36] presumably involving a decreased pK_a of His18 in the Z domain upon binding. This is because the binding is somewhat weaker at the lower pH (where a histidine residue exposed to water is expected to be protonated) and because the difference in ΔH°_{bind} (-1 kcal mol^{-1}) corresponds within error to the expected exothermic uptake of one proton by phosphate buffer. However, the control experiment in Tris buffer for which the ioinization enthalpy is much larger than that in phosphate buffer (11.3 vs 1 kcal mol^{-1}, respectively) shows that any linked protonation effect is small at pH 7.25. The measured difference of a -2 kcal mol^{-1} more exothermic reaction in Tris buffer would correspond to an average protonation shift of 0.2 H^+. The small magnitude of any possible effect and the fact that the data is obtained using phosphate buffer therefore excludes the possibility that the binding thermodynamics data are contamined by linked buffer protonation effects.

The change in heat capacity upon binding is the same within experimental error for pH 5.7 and pH 7.25 (-370 to -400 cal mol^{-1} K^{-1}) and somewhat smaller in the presence of TMAO (-310 cal mol^{-1} K^{-1}). The temperature dependence of the binding affinity, finally, is in all cases small and hardly resolved in the investigated temperature range. This is because the $\Delta C^{\circ}_{P,bind}$ values are moderate and because the measurements are made at temperatures close to T_H, where the temperature dependence of the affinity is zero as it goes through its optimum value.

Secondary Structure Content of Z_{SPA-1} in Free and Bound States. The formation of a Z:Z_{SPA-1} complex results in a significant increase in the average helicity of Z_{SPA-1} as illustrated in Figure 4, in which CD spectra of the interacting components and the complex are compared. All spectra show negative minima at 208 and 222 nm and changes sign from negative to positive at 202 nm, and these are the characteristic features of predominantly helical secondary structure. However, the magnitude of the CD signal of MG state Z_{SPA-1} is significantly smaller than that of the Z domain (as noted previously), and it is also smaller than the CD measured for the Z:Z_{SPA-1} complex. It is possible to calculate the contribution from Z_{SPA-1} to the CD of the complex, because the secondary structure content of Z does not change upon complex formation. The Z:Z_{SPA-1} sample for which the CD spectrum is shown in

(36) Baker, B. M.; Murphy, K. P. *Biophys. J.* **1996**, *71*, 2049−2055.

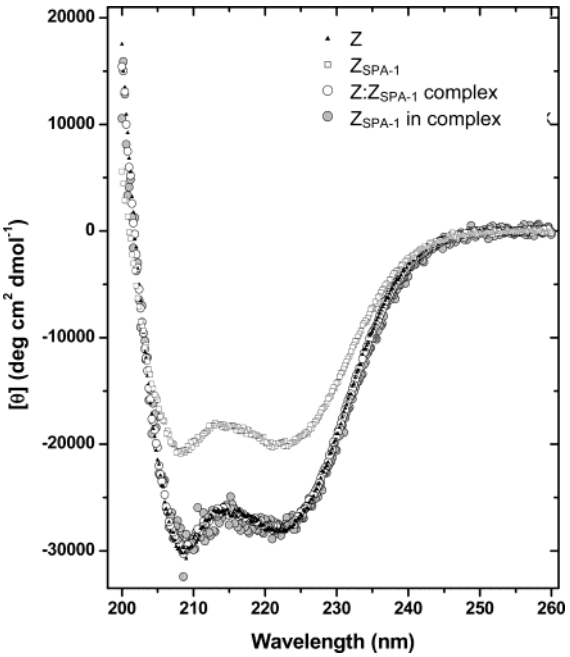

Figure 4. Circular dichroism (molar ellipticity) of Z (▲), Z_{SPA-1} (□), and the Z:Z_{SPA-1} complex (○). The CD of Z_{SPA-1} in the complex (filled gray circle) was calculated as described in the text. The data are from measurements in 20 mM phosphate buffer at pH 5.7 and (total) protein concentrations of 25 to 35 μM.

Figure 4 contained 25 μM Z and 10 μM Z_{SPA-1}, where the excess of Z was motivated to optimize the fraction of bound Z_{SPA-1}. The fact that a small fraction of Z_{SPA-1} is not bound (7% since K_d = 1.2 μM) was considered in the calculations, but the presence of an insignificantly small fraction (3%) of unfolded Z_{SPA-1} at 20 °C was neglected. The calculated CD signal of Z_{SPA-1} in the complex is virtually identical to that of the Z domain (Figure 4) as expected from the observed secondary structure of the complex.[19] The difference between the CD of free and bound Z_{SPA-1} demonstrates a conformational stabilization of helical secondary structure, which we quantify and discuss further below.

Discussion

MG State Z_{SPA-1} Comformation Is Entropically Unfavorable. The native state of the Z_{SPA-1} affibody in the absence of the Z domain is a state which is conformationally reminiscent of a molten globule as discussed in the Introduction. The thermal unfolding data of Z and Z_{SPA-1} presented here allows for a thermodynamic interpretation of the structural differences. The analysis of thermal stability of Z in the absence of denaturant is not highly precise due to the high melting temperature (T_m of ca. 80 °C), but a comparison of the values obtained at the different GuaHCl concentrations shows that the folding reaction is enthalpy driven, involves a heat capacity change on the order of −300 to −400 cal mol^{-1} K^{-1}, and results in a total stabilization of ca. 5 kcal mol^{-1} at 25 °C. These values are not untypical for a small globular protein, as judged by comparison of data compiled by Felitsky and Record.[35] The folding stability of Z_{SPA-1} in the free MG state is significantly lower than that of the parental Z domain with T_m = 42 °C and ΔG°_{unfold} = 1.7 kcal mol^{-1}. The analysis indicates that the folding enthalpy is favorable and perhaps even more favorable than in the case of the Z domain but that a significant thermodynamic difference between the two proteins also exists due to an almost immeasurably small heat capacity change (100 cal mol^{-1} K^{-1} or less) for unfolding of Z_{SPA-1}. The heat capacity change in protein folding is closely related to changes in water-accessible polar and nonpolar surface area resulting from the formation of a well packed hydrophobic core which is not accessible to water. An inspection of the structure of Z_{SPA-1} in complex with Z shows that optimal core packing and protection from water are not possible if not all three helices are simultaneously present. The structural data that indicate incomplete helix formation and/or local unfolding events in helices 1 and 2 and other biophysical evidence for molten globule-like behavior in Z_{SPA-1} are therefore consistent with the observed folding thermodynamics which suggest that the hydrophobic core is not completely packed and/or solvent exposed in the affibody.

Possible Thermodynamic Basis for Suboptimal Binding of Z_{SPA-1} to Z. The size of phage-displayed affibody libraries (on the order of 10^7 phages) is small compared to the number of possible mutants ($\sim 10^{17}$), and this puts obvious limits on the possibilities that the optimal binding proteins are present in a single library. Strong binding with K_d values in the nanomolar range has still been observed.[15] It is therefore clear that neither the relatively small size of the three-helix domain nor the fact that a limited area of the total surface (13 residues) is randomized in the phage-displayed library are a priori limiting for strong binding. This conclusion is also supported by the observation that second-phase selection, or so-called "affinity maturation", of affibodies can result in selection of much improved binders.[15,16] However, most (publicly available) work on affibodies describe the identification of binding proteins with affinities in the range 10^{-7} to 10^{-5} M. This is also the case with Z_{SPA-1}; the Z:Z_{SPA-1} complex is about 2 to 3 orders of magnitude weaker than the strongest affibody:target complexes, and also compared to the Z domain:Ig-Fc complex.[37] Apart from the use of Z:Z_{SPA-1} as a model for protein−protein interactions, it might therefore also be important for engineering of binding proteins to understand the structural basis for the fact that the binding is not stronger. As a starting point for the discussion, one can identify three possible sources for loss of free energy of strong (nanomolar) binding in the case of Z_{SPA-1}: (i) the decreased thermal stability, which requires folding of a significant fraction of the ensemble at room temperature and as much as 15% at 30 °C and pH 7.25 (K_{unfold} = 0.14; Table 2), (ii) the fact that the binding interface in some way is suboptimal, or (iii) the fact that the folded Z_{SPA-1} is in a molten-globule-like state for which a conformational stabilization to form the three full helices and a completely packed core is required upon binding to Z.

It would in principle also be possible that self-association of Z_{SPA-1} results in weaker binding and that the disruption of Z_{SPA-1} aggregates also contributes to the observed enthalpy of folding and binding. Z_{SPA-1} is known to self-associate at high concentrations at which the CD spectrum changes, but there are no significant indications of such effects at concentrations below 50 μM.[19] An unmeasurably small fraction of self-associated Z_{SPA-1} cannot be completely ruled out because gel filtration of 100 μM Z_{SPA-1} samples suggests a somewhat larger

(37) Starovasnik, M. A.; Braisted, A. C.; Wells, J. A. *Proc. Natl. Acad. Sci. U.S.A.* **1997**, *94*, 10080−10085.

average molecular weight than (monomeric) Z samples.[24] However, as the dissociation constant for the Z_{SPA-1} self-association equilibrium appears to be in the millimolar range, the expected effects on the binding affinity are negligible. Furthermore, the possibility that the disruption of a small fraction of self-associated Z_{SPA-1} present at 50 μM accounts for the excess exothermic binding enthalpy at higher binding enthalpies would imply that the thermodynamics of disruption of aggregates is identical to the thermodynamics that we attribute to Z_{SPA-1} folding. This is unlikely, in particular when considering that the binding enthalpy correction is much smaller in the presence of TMAO, whereas TMAO has little or no effect on the self-association observed at higher concentrations.[24]

Thermal Instability of Z_{SPA-1} Has Only a Small Effect on Binding Affinity. With regard to the first source of Z_{SPA-1} "misbehavior", that the shift of the MG state unfolding equilibrium at higher temperature (30 °C) results in a weaker complex than binding of a folded Z_{SPA-1} ensemble at low temperature or in the presence of TMAO, there is clearly an effect, but it is not very large. The data in Table 2 show that the apparent binding affinity at 30 °C is improved by only about 10% (pH 7.25) to 20% (pH 5.7) when the process of binding is thermodynamically separated from the shift in the unfolding equilibrium. A somewhat larger effect is observed when comparing binding in buffered water (at pH 7.25) to binding in the presence of 1 M TMAO, in which case the apparent dissociation constant drops from 1 μM to 0.5 μM at 30 °C or from ca. 0.7 μM to 0.25 μM at 20 °C. However, part of the effect of the added osmolyte appears to result from some mechanism related to complex formation rather than to the action of the cosolvent to stabilize Z_{SPA-1}. This is because K_d values that have been corrected for coupled folding indicate stronger binding in both TMAO and betaine-containing solutions than in phosphate buffer at pH 7.25. The molecular origin for the effect of TMAO and betaine on binding might or might not resemble the effect that is observed on protein folding,[38,39] but it is small and not completely resolved and therefore not discussed further. Hence, we conclude that thermal instability of MG state of Z_{SPA-1} is not the primary explanation for weak binding. Simple insertion of numbers into eq 10 shows that a value of $K_{unfold} = 1$ (50% unfolded Z_{SPA-1}) only would reduce the apparent binding affinity by 50%. In fact, to account for an apparent binding affinity of 1 μM for coupled folding and binding with a (corrected) $K_{d,bind} = 10$ nM for binding, one would need a thermal instability corresponding to $K_{unfold} = 100$ (99% unfolded).

Structure of the Z:Z_{SPA-1} Interface Is Inconspicuous. A suboptimal binding interface is obviously a potential explanation for weak binding. To assess if the interaction interface in the Z:Z_{SPA-1} complex in any way appears to lack features signifying strong binding we compared it to structural statistics for other known protein−protein complexes and also calculated the expected thermodynamics for binding of a (hypothetic) ordered three-helix bundle Z_{SPA-1}. Lo Conte et al. analyzed a large number of structural parameters in 75 protein−protein complexes of known three-dimensional structure.[40] According to this analysis there is a standard-size interface in 52 of the 75 complexes in which a 1600 (±400) Å^2 total surface area is buried. The corresponding buried surface in the Z:Z_{SPA-1} complex is 1632 Å^2. Other structural parameters of the Z:Z_{SPA-1} are also similar to average values. These include the number of hydrogen bonds at the interface (10 in Z:Z_{SPA-1}; average of 10.1 (±4.8) in 75 complexes[40]), the fraction nonpolar compared to polar or charged interactions at the interface (64% in Z:Z_{SPA-1}; 56 ± 6% in the average complex), and number of interface atoms (186 in Z:Z_{SPA-1}; 211 ± 81 average). It is therefore difficult to point out any specific discrepancy of the Z:Z_{SPA-1} interface that would signify a complexation that is weaker than in protein−protein complexes for which dissociation constants in the range pM to nM have been measured, as judged by a comparison of structural data compiled by Lo Conte et al.[40] and stability data compiled by Brooijmans et al..[41]

It is not, in general, possible to a priori relate the structure and interactions observed at a protein−protein interface to a free energy of binding with a precision sufficient to resolve dissociation constants of 10 nM as compared to 1 μM, corresponding to a free energy difference of 2.7 kcal mol^{-1}. However, significant progress has been made for protein complexes where the structures of all interacting components in both free and complexed states are known. For instance, Lavigne et al. used the structure-based approach described in the Methods section to calculate a dissociation constant (40 pM) for the complex between microcystin-LR and the catalytic domain of protein phosphatase-1 which is in excellent agreement with the experimental value (39 pM).[10] Similarily, Horn et al. used high-resolution X-ray structures to compute thermodynamic parameters for binding of the OMTKY3 serine protease inhibitor to two serine proteases. They obtained values of ΔC_P° that are correct within the limits of experimental uncertainty (ca 100 cal mol^{-1} K^{-1}) and values of ΔH°, $-T\Delta S^\circ$, and ΔG° which in all cases fall within 1 to 4 kcal mol^{-1} of observed values and significantly less when conformational dynamics was considered.[9] A similar analysis of the Z:Z_{SPA-1} complex is not possible, because the free (MG state) Z_{SPA-1} appears to adopt multiple interconverting conformations. However, it is interesting to compare the observed binding thermodynamics to what would be expected under the assumption that the structures of free and complexed Z_{SPA-1} were identical, because this comparison might point to effects that can be traced to the conformational stabilization that occurs in Z_{SPA-1} upon binding.

Hence we calculated expected ΔC_p, ΔH°, and $-T\Delta S^\circ$ values for Z:Z_{SPA-1} binding using the parametrization of changes in solvent accessible surfaces areas and conformational entropy developed by Freire, Murphy, and co-workers (descibed in the Methods section). The calculations were carried out for 10 structural models in each of the PDB entry files for Z (ref 25; 1Q2N.pdb and Z:Z_{SPA-1} (ref 19; 1H0T.pdb) to assess the precision of the output and to allow for a better sampling of possible free and bound state conformations. The free Z_{SPA-1} structure was in all cases assumed to be the same as in the corresponding Z:Z_{SPA-1} complex. Hence, for a *hypothetical* complex formation, in which the structures of free and bound Z_{SPA-1} are identical, we obtain average values of $\Delta C_P^\circ = -394$ cal mol^{-1} K^{-1} (range of −331 to −484 cal mol^{-1} K^{-1}), ΔH°

(38) Bolen, D. E.; Baskakov, I. V. *J. Mol. Biol.* **2001**, *310*, 955−963.
(39) Zou, Q.; Bennion, B. J.; Daggett, V.; Murphy, K. P. *J. Am. Chem. Soc.* **2002**, *124*, 1192−1202.
(40) Lo Conte, L.; Chothia, C.; Janin, J. *J. Mol. Biol.* **1999**, *285*, 2177−2198.
(41) Brooijmans, N.; Sharp, K. A.; Kuntz, I. D. *Proteins: Struct., Funct., Genet.* **2002**, *48*, 645−653.

$= 0.2$ kcal mol^{-1} (-5.9 to $+5.5$ kcal mol^{-1}), and $-T\Delta S° = -22.9$ kcal mol^{-1} (-18.6 to -28.5 kcal mol^{-1}) for binding at 25 °C. Comparing these to the experimental parameters in Table 3, we find that the ranges of calculated values for $\Delta C_P°$ and $\Delta H°$ include the experimental values but that the calculations significantly overestimate the favorable entropic contributions to binding; the observed values of $-T\Delta S°_{bind}$ range from -1 to -5 kcal mol^{-1}. The conformational adaptation, or induced fit, of the Z domain surface is considered in the calculations, since we used the free Z structure as reference, and the discrepancy in the calculated binding entropy is therefore likely due to that conformational stabilization in Z_{SPA-1} upon binding is not considered.

Conformational Stabilization of Z_{SPA-1} Is Associated with an Unfavorable Entropy Change. An indication from experimental data of the magnitude of the conformational entropy penalty can be obtained from a comparison of the observed average helicity in free Z_{SPA-1} to what is observed in the Z:Z_{SPA-1} complex. Inserting the value $[\theta]_{obsd} = -20\,500$ deg cm^2 dmol^{-1} for Z_{SPA-1} and $-29\,500$ deg cm^2 dmol^{-1} for the Z domain at 10 °C (Figure 1) in eq 1, we obtain fractional helicities $f_H = 55\%$ (32 residues in α-helical conformation) for Z_{SPA-1} and $f_H = 77\%$ (45 helical residues) for Z. The latter value corresponds rather well to the helicity calculated from the structure (PDB entry 1Q2N.pdb) in which 44 of 58 residues adopt an α-helical conformation. In the NMR structure of the Z:Z_{SPA-1} complex, there are 41 helical residues in α-helical conformation and an additional three residues in a 3_{10}-helix conformation in Z_{SPA-1}. We can therefore expect that the conformational entropy loss associated with the stabilization of the free MG state into the bound state structure corresponds to folding of 12 residues from random coil conformation into a helical conformation. D'Aquino et al. measured $\Delta S_{ex\rightarrow u}$ and ΔS_{bb} values (see description of eq 14) for helix unfolding for all amino acids except proline in the context of two different pairs of mutants of a peptide corresponding to the leucine zipper region of GCN4. NMR data on free Z_{SPA-1} shows that helix III in free Z_{SPA-1} is stable and that helices I and II are transiently formed.[24] The observed loss of helicity in Z_{SPA-1} is therefore an average and it is not possible to identify any specific region or fragment in which conformational change occurs. However, an estimate of the effect can be obtained as an expected average for the different residues present in helices 1 or 2. The value for $\Delta S_{ex\rightarrow u} + \Delta S_{bb}$ thus obtained from the D'Aquino data is 4.6 cal (mol residues)$^{-1}$ K^{-1} (for unfolding), and it corresponds to an unfavorable conformational entropy contribution (for folding) of 16 kcal mol^{-1} at 25 °C (helix formation of 12 residues) and an even more unfavorable value if additional residues in the loop connecting helices 1 and 2 in Z_{SPA-1} also become conformationally restricted in the complex.

Another way to estimate the conformational contribution to the binding entropy is provided by an analysis based on the assumption that the entropies of both nonpolar[42] and polar desolvation[43] are zero at 385 K. (This is equivalent to stating that both the reference temperatures in eq 13 are 385 K.) With this assumption, the conformational entropy change can be calculated directly from the measured binding entropy and heat capacity change, without a priori estimates of surface area changes, as

$$-\Delta S_{conf} = \Delta S_{solv}(T) + \Delta S_{rt} - \Delta S°_{bind}(T) = \Delta C_{P,bind} \ln\left(\frac{T}{385}\right) + \Delta S_{rt} - \Delta S°_{bind}(T) \quad (15)$$

Given experimental values at pH 7.25 of $\Delta C_{P,bind} = -370 \pm 20$ cal mol^{-1} K^{-1}, $\Delta S°_{bind} = 9.1 \pm 0.3$ cal mol^{-1} K^{-1} at 25 °C, and $\Delta S_{rt} = -8$ cal mol^{-1} K^{-1} as before, we obtain $\Delta S_{conf} = -78 \pm 6$ cal mol^{-1} K^{-1}, corresponding to $-T\Delta S_{conf} = 23 \pm 2$ kcal mol^{-1} at 25 °C. This number is comparable to that obtained from calculations based on changes in helicity. It also coincides with the entropy descrepancy that is obtained in the structure-based calculations assuming binding of a hypothetical Z_{SPA-1} that assumes the bound-state structure. We therefore conclude that the stabilization of the MG state of free Z_{SPA-1} to an ordered three-helix structure in the complex is associated with a significant conformational entropy penalty.

Desolvation Forces and Binding Heat Capacity. So what then drives the formation of the Z:Z_{SPA-1} complex? An obvious contribution comes from the desolvation forces, i.e., the hydrophobic effect. Water is relieved from constraining surfaces upon complex formation, and presumably also as the conformation of Z_{SPA-1} changes from the MG state to the bound-state structure, and this effect contributes very favorably to the entropy of binding. The magnitude of the desolvation entropy at 25 °C can be estimated (as described above) to $-T\Delta S_{solv} = -T\Delta C_{P,bind} \ln(T/385) = -28$ kcal mol^{-1}.

It should in principle be possible to separate and compare the contributions to the desolvation effect originating from the events of stabilization and binding of a stabilized conformation by analyzing the heat capacity changes. This is because the heat capacity change for conformational change is the difference between the experimentally observed $\Delta C°_{P,bind}$ and the value obtained from the structure-based calculations for binding of Z_{SPA-1} with a preformed bound-state structure. However, both these values fall close to -400 cal mol^{-1} K^{-1}, and the uncertainties in the structure-based calculations appear to be on the order of 200 cal mol^{-1} K^{-1}. It is therefore not possible to resolve the heat capacity of conformational change in Z_{SPA-1} experimentally. One might speculate that a significant fraction of the desolvation effect comes from the complex formation as suggested by structure-based calculations. Some contribution from the conformational stabilization is also likely, as suggested by a comparison of unfolding thermodynamics of Z_{SPA-1} and the Z domain: both domains appear to be well structured in the complex, and a high degree of order is associated with a low heat capacity, but the free Z domain unfolds with a $\Delta C°_{P,unfold}$ of ca. 400 cal mol^{-1} K^{-1}, whereas the heat capacity change for thermal unfolding of the MG state Z_{SPA-1} is smaller. It is reasonable to assume that the "lack" of heat capacity observed for Z_{SPA-1} unfolding instead should appear as a consequence of the ordering and desolvation that accompanies the transition to a more ordered structure upon binding. However, the uncertainties associated with the calculations and the experimental determination of $\Delta C°_{P,unfold}$ for Z_{SPA-1} prohibit a quantitative assessment of the fractions of the total expected heat capacity change associated with the transition from a fully unfolded state to the MG state and from the MG state to the ordered bound-state conformation, respectively.

(42) Baldwin, R. L. *Proc. Natl. Acad. Sci. U.S.A.* **1986**, *83*, 8069−8073.
(43) Murphy, K. P.; Freire, E.; Paterson, Y. *Proteins: Struct., Funct., Genet.* **1995**, *21*, 83−90.

Binding Enthalpy. The $Z:Z_{SPA-1}$ binding enthalpy is favorable for complex formation, and it constitutes about half of the binding free energy at room temperature. Favorable binding enthalpies (at 25 °C) are in fact observed with most specific protein−protein interactions (some protease-inhibitor complexes are examples of exceptions) and apparently without exception in antibody−antigen complexes (see for instance ref 1 for a review and also refs 44 and 45 and work cited therein). The magnitude of the binding enthalpy in the case of $Z:Z_{SPA-1}$ (−5.5 kcal mol^{-1}) appears to be smaller than that in peptide−antibody complexes, where values −15 kcal mol^{-1} or lower are frequent, but the range of values observed and the uncertainties with regard to buffer effects that accompany some of the literature data[1] unfortunately exclude any further discussion about whether $Z:Z_{SPA-1}$ is thermodynamically more similar to an antibody−peptide complex than to other protein−protein complexes. The observed binding enthalpy is consistent with a number of specific interactions at the $Z:Z_{SPA-1}$ interface, for instance 10 hydrogen bonds. However, enthalpically favorable hydrogen bonding is also expected when secondary structure is formed in bound-state Z_{SPA-1}, as well as a consequence of desolvation and electrostatic effects.

Acknowledgment. This work was supported by the Swedish Research Council. We appreciate discussions with Prof. Per-Åke Nygren at the Department of Biotechnology at KTH.

JA047727Y

(44) Welfle, K.; Misselwitz, R.; Sabat, R.; Volk, H. D.; Schneider-Mergener, J.; Reineke, U.; Welfle, H. *J. Mol. Recognit.* **2001**, *14*, 89−98.
(45) Welfle, K.; Misselwitz, R.; Höhne, W.; Welfle, H. *J. Mol. Recognit.* **2003**, *16*, 54−62.